tvst

Article

Xeno- and Feeder-Free Differentiation of Human iPSCs to Trabecular Meshwork-Like Cells by Recombinant Cytokines

Wenyan Wang[1,2,*], Yongzhen Miao[1,*], Shangru Sui[1], Yanan Wang[1,2], Shen Wu[3], Qilong Cao[4], Haoyun Duan[5], Xia Qi[5], Qingjun Zhou[5], Xiaojing Pan[5], Jingxue Zhang[3], Xuehong Chen[2], Yantao Han[2], Ningli Wang[3], Markus H. Kuehn[6,7], and Wei Zhu[1,8]

[1] Department of Pharmacology, School of Pharmacy, Qingdao University, Qingdao, China
[2] School of Basic Medicine, Qingdao University, Qingdao, China
[3] Beijing Institute of Ophthalmology, Beijing Tongren Hospital Eye Center, Beijing, China
[4] Qingdao Haier Biotech Co. Ltd., Qingdao, China
[5] Qingdao Eye Hospital, Shandong Eye Institute, Shandong Academy of Medical Sciences, Qingdao, China
[6] Department of Ophthalmology and Visual Sciences, University of Iowa, Iowa City, IA, USA
[7] Center for the Prevention and Treatment of Visual Loss, Iowa City Veterans Affairs Medical Center, Iowa City, IA, USA
[8] Advanced Innovation Center for Big Data-Based Precision Medicine, Beijing University of Aeronautics and Astronautics-Capital Medical University, Beijing, China

Correspondence: Wei Zhu, Department of Pharmacology, School of Pharmacy, Qingdao University, 38 Dengzhou Road, Qingdao 266021, Shandong, China. e-mail: wzhu@qdu.edu.cn

Received: August 6, 2020
Accepted: March 1, 2021
Published: May 20, 2021

Keywords: induced pluripotent stem cells; trabecular meshwork; differentiation; recombinant cytokines

Citation: Wang W, Miao Y, Sui S, Wang Y, Wu S, Cao Q, Duan H, Qi X, Zhou Q, Pan X, Zhang J, Chen X, Han Y, Wang N, Kuehn MH, Zhu W. Xeno- and feeder-free differentiation of human iPSCs to trabecular meshwork-like cells by recombinant cytokines. Transl Vis Sci Technol. 2021;10(6):27, https://doi.org/10.1167/tvst.10.6.27

Purpose: Stem cell-based therapy has the potential to become one approach to regenerate the damaged trabecular meshwork (TM) in glaucoma. Co-culture of induced pluripotent stem cells (iPSCs) with human TM cells has been a successful approach to generate autologous TM resembling cells. However, the differentiated cells generated using this approach are still problematic for clinical usage. This study aimed to develop a clinically applicable strategy for generating TM-like cells from iPSCs.

Methods: Highly expressed receptors during iPSC differentiation were identified by AutoSOME, Gene Ontology, and reverse transcription polymerase chain reaction (RT-PCR) analysis. The recombinant cytokines that bind to these receptors were used to generate a new differentiation protocol. The resultant TM-like cells were characterized morphologically, immunohistochemically, and transcriptionally.

Results: We first determined two stages of iPSC differentiation and identified highly expressed receptors associated with the differentiation at each stage. The expression of these receptors was further confirmed by RT-PCR analysis. Exposure to the recombinant cytokines that bind to these receptors, including transforming growth factor beta 1, nerve growth factor beta, erythropoietin, prostaglandin F2 alpha, and epidermal growth factor, can efficiently differentiate iPSCs into TM-like cells, which express TM biomarkers and can form dexamethasone-inducible CLANs.

Conclusions: We successfully generated a xeno- and feeder-free differentiation protocol with recombinant cytokines to generate the TM progenitor and TM-like cells from human iPSCs.

Translational Relevance: The new approach minimizes the risks from contamination and also improves the differentiation efficiency and consistency, which are particularly crucial for clinical use of stem cells in glaucoma treatment.

Introduction

Intraocular pressure (IOP) homeostasis, which is dramatically influenced by the resistance to aqueous humor (AH) drainage,[1] is essential for ocular health. Disruption of the trabecular meshwork (TM) function can lead to increased resistance to AH outflow and sustained elevation of IOP, which is the major risk factor for glaucomatous optic neuropathy.[2,3] Multiple

groups have demonstrated that stem cell-based therapy is one effective approach to regenerate the damaged TM and maintain the IOP in the eye; such approaches have included the use of adult TM stem cells, mesenchymal stem cells, and induced pluripotent stem cells (iPSCs).[4–12]

To date, the most commonly used approach to generate TM-like cells from iPSCs is through co-culture of iPSCs with human TM (HTM) cells.[13] Using cell culture medium conditioned by human TM cells, Abu-Hassan et al.[10] successfully generated TM-like cells from iPSCs growing on a TM cell-secreted extracellular matrix. Likewise, our group demonstrated that iPSCs growing on Matrigel-coated plates can also be induced to differentiate into TM-like cells by co-culturing iPSCs with human immortalized TM cells.[13] We subsequently improved differentiation by using HTM cells, a differentiation approach that appears to be more successful than the use of human immortalized TM cells according to the morphology of differentiated iPSCs.[9]

Although with these improvements, these iPSC-derived TM-like cells are still problematic for clinical usage because of contamination from both fetal bovine serum (FBS) and humans, unstable differentiation efficiency, and the required long-term culture in vitro. FBS commonly used for expending cells in vitro and the products from other human beings could carry the risk of xenoimmunization and zoonotic transmission.[14] Human TM cells from different donors exhibit some differences in cell viability and function,[15] which can lead to unstable efficiency for stem cell differentiation. Long-term cell culture in vitro triggers many side effects, such as genetic mutation[16] and cellular senescence.[17] To circumvent these disadvantages, a new differentiation approach of xeno- and feeder-free culture eliminating various contaminations is required.

Here, we first defined two stages of iPSC differentiation through morphological analysis and bioinformatic analysis of RNA-sequencing data of TM-like cells.[9] From each stage, highly expressed receptors associated with TM development were selected through AutoSOME (http://jimcooperlab.mcdb.ucsb.edu/autosome) and Gene Ontology analysis, further confirmed by reverse transcription polymerase chain reaction (RT-PCR) analysis. Recombinant cytokines binding to these receptors were used to generate the new xeno- and feeder-free differentiation approach, which can effectively induce human iPSCs to differentiate into TM-like cells, by studying their morphological features and conducting immunohistochemistry analyses and transcriptomic assays.

Material and Methods

Human Trabecular Meshwork Cell Isolation and Culture

Ocular anterior segments from human donors 1 to 3 were obtained from the Iowa Lions Eye Bank (Iowa City, IA), and those from donors 4, 5, and 6 were obtained from Beijing Tongren Eye Hospital (Beijing, China). The protocol for collecting human tissues was approved by the institutional review boards of the University of Iowa Institutional and Beijing Tongren Eye Hospital. After dissection, the TM was visible as a brown circle in the irideocorneal angle and isolated by using a 0.5-mm curette. After rinsing with Dulbecco's modified eagle medium (DMEM; Sigma-Aldrich, St. Louis, MO), the tissue was digested in DMEM containing 4 mg/mL collagenase A (Sigma-Aldrich) and 4 mg/mL human serum albumin (Sigma-Aldrich) at 37°C for 2 hours. After centrifugation (1000 rpm for 3 minutes), the pellets were resuspended in TM cell growth medium comprised of Gibco Medium 199E containing 20% Gibco FBS, 90 µg/mL porcine heparin (Sigma-Aldrich), 20 U/mL endothelial cell growth supplement (Sigma-Aldrich), and 1.7 mM L-glutamine (Sigma-Aldrich). The digested tissue was seeded onto 1% gelatin precoated six-well plates (Thermo Fisher Scientific, Waltham, MA) and cultured in the incubator with 5% CO_2 at 37°C. As in our previous studies,[8] cells at passages five to eight with robust expression of TM biomarkers and the capacity for dexamethasone (DEX)-induced myocilin (MYOC) secretion were used in this study.

Human iPSC Generation and Culture

Human induced pluripotent stem cells were created through reprogramming of renal urethra epithelial cells isolated from the urine of three healthy human donors, designated U1, U2, and U3 (Cellapy Biotechnology, Beijing, China).[18] Renal urethra epithelial cells at passage two were infected with non-integrating Sendai virus carrying Oct4, Sox2, c-Myc, and Klf4 transcription factors (CytoTune-iPS 2.0 Sendai Reprogramming Kit; Thermo Fisher Scientific). Successfully reprogrammed cells, iPSC colonies, were generated during days 9 to 28 after infection and were transferred for expansion. Written informed consent was obtained from all donors, and the protocol to reprogram renal cells was carried out following the guidelines for stem cell clinical research in China. The reprogramming was accomplished by using the CytoTune-iPS 2.0 Sendai Reprogramming Kit, and the reprogrammed cells were

cultured in mTeSR-1 Standarized Medium containing recombinant human basic fibroblast growth factor (rh-bFGF) and recombinant human transforming growth factor beta (rh-TGF-β; STEMCELL Technologies, Cambridge, MA) in 0.2% Matrigel (Corning Inc., Corning, NY) precoated six-well plates. The iPSC colonies were then isolated by using 5 mg/mL collagenase (Sigma-Aldrich) and expanded in mTeSR-1 Standardized Medium (STEMCELL Technologies) as described previously.[18] The iPSCs at passages 20 to 30 were tested as the Sendai virus-free cells and used for the differentiation.

Human iPSC Differentiation by Conditioned Medium

Human iPSCs derived from the renal cells of U1, U2, and U3 were seeded on 0.2% Matrigel-coated plates and cultured in mTeSR-1 Standardized Medium until reaching 5% to 10% confluency. Human TM cells from each donor were seeded at 70% to 90% confluency in Corning Transwell cell culture plate inserts and positioned above the human iPSCs. These cells were cultured in biopsy medium comprised of Minimum Essential Medium-α (MEM-α; Thermo Fisher Scientific), 10% FBS, and 0.2% Primocin (InvivoGen, San Diego, CA). The inserts with human TM cells from different individuals were switched routinely to ensure that iPSCs were exposed to conditioned medium from all three human donors.

Enzyme-Linked Immunosorbent Assay Analysis

Human TM cells (5×10^4) were seeded in one well of a 96-well plate and cultured in the TM medium until reaching 100% confluency. The supernatant was collected for enzyme-linked immunosorbent assays (ELISAs). First, the capture antibodies with specificity for TGF-β_1, nerve growth factor beta (NGF-β), erythropoietin (EPO), epidermal growth factor (EGF), or prostaglandin F2 alpha (PGF2α) were immobilized in microtiter wells (Shanghai BlueGene Biotech Co., Ltd., Shanghai, China). Conditioned medium and standard samples at 0, 3, 6, 12, 24, and 48 pg/mL were incubated with the immobilized antibodies at 37°C for 60 minutes. After washing with wash buffer (Shanghai BlueGene Biotech) five times, the second specific antibodies conjugated to horseradish peroxidase (Shanghai BlueGene Biotech) were added to react with the captured cytokine. A chromogenic substrate (Shanghai BlueGene Biotech) was then added and incubated at 37°C for 15 minutes. After termination, the optical density of the reaction was measured with a spectrophotometer (Synergy MxMulti-Mode Microplate Reader; BioTek, Winooski, VT) and compared with the readings of standard samples. The experiment was repeated three times by using the HTM cells of three donors.

Xeno- and Feeder-Free Differentiation With Recombinant Cytokines

Human iPSCs derived from the renal cells of U1, U2, and U3 were seeded in 0.2% Matrigel-coated plates and cultured in mTeSR-1 Standardized Medium until reaching 5% to 10% confluency. Human iPSCs were then cultured in stage 1 differentiation medium containing MEM-α, 10% KnockOut Serum Replacement (Thermo Fisher Scientific) and 2 ng/mL TGF-β_1, 100 ng/mL NGF-β, and 2 U/mL EPO (Sino Biological, Beijing, China) for 7 days. Subsequently, the cells were maintained for 14 days in stage 2 differentiation medium comprised of MEM-α, 10% KnockOut Serum Replacement, 2 ng/mL TGF-β_1, 100 ng/mL NGF-β, 2 U/mL EPO, 10 µM PGF2α, and 10 ng/mL EGF. KnockOut Serum Replacement is a commercial cell culture additive[19,20] that has been proved to be an effective serum substitute for a number of mammalian cells cultured in vitro. The medium was changed every 2 days. The morphology of differentiated cells was monitored by an inverted microscope (Leica Microsystems, Wetzlar, Germany).

RNA Sequencing and AutoSOME Analysis

RNA sequencing was carried out in human fibroblasts, fibroblast-derived iPSCs, and conditioned medium-derived TM-like cells for 1, 2, and 3 months and in human TM cells of donors 1 to 3 on the HiSeq 2500 sequencer (Illumina, San Diego, CA). We also collected urine epithelial cell-derived iPSCs, urine-derived TM-like cells by conditioned medium (U-TM-like cells-C; 1 month differentiation), urine-derived TM-like cells by a xeno-free approach (U-TM-like cells-X), and HTM cells of donors 4 and 5 for RNA sequencing using the Illumina NovaSeq 6000 System. Total RNA was extracted using TRIzol (Thermo Fisher Scientific) and assessed using Agilent 2100 Bioanalyzer (Agilent Technologies, Santa Clara, CA) and Qubit Fluorometer (Thermo Fisher Scientific). A stranded mRNA library was prepared for sequencing mRNA and generating stranded mRNA information. The fragments per kilobase per million mapped reads (FPKM) value, which reflects the relative expression of a transcript, was compiled from the Cufflinks output (University of Washington, Seattle, WA). Genes with fold change > 4 and averaged FPKM > 1

Table 1. Primers for Amplifying Receptors

Gene	Forward Primer	Reverse Primer
HEPOR	CTTGTGGTATCTGACTCT	ATAAGGCTGTTCTCATAAG
HTGFBR1	GATTACCAACTGCCTTAT	TTAGCCATTACTCTCAAG
HTGFBR2	GAATATAACACCAGCAATC	CAGTAGAAGATGATGATGA
HTGFBR3	GTCTACTATAACTCCATTGT	TCTCCTTCATCCATATCT
PTPRN	AGTGAAGGAGATTGACAT	CAAATTCAAACTGGTCCT
PTGER4	TGGTCATCTTACTCATTG	GCATTTCTCTTGTATGTATAG
PTGFR	AATGATGTTAAGTGGTGT	ATGTCTTCTGTGTTGTAG
PTGER2	ATGAATGAAACCTCTTCC	CATCTTGTGTTCTTAATGAA
PTGER1	CTTGTCGGTATCATGGTG	GTAGGATGTACACCCAAG
EDIL3	AGTTACTGGTGTGATTAC	TCATTACTGTAGGCAATT
MEGF9	GTCATCATCATTGTTGTG	CTTCATTGCCATCATCTT

EDIL3, EGF-like repeat and discoidin I-like domain-containing protein 3; *HEPOR*, human erythropoietin receptor; *HTGFBR1*, 2, and 3, human transforming growth factor-β receptor 1, 2, and 3; *MEGF9*, multiple epidermal growth factor-like-domains 9; *PTGER1*, 2, and 4, prostaglandin E receptor 1, 2, and 4; *PTGFR*, prostaglandin F2-alpha receptor; *PTPRN*, protein tyrosine phosphatase receptor-type N.

were selected for AutoSOME analysis.[21] Unit variance, median centering, and P threshold of <0.01 were chosen in AutoSOME for clustering genes with the same expression modulus. Cluster analysis (CapitalBio Technology Co., Ltd., Beijing, China) was performed using significantly differentially expressed genes with fold differences ≥ 2 ($|\log2FC| \geq 1$, where FC is the fold change of expressions) and $P < 0.05$.[22]

RT-PCR Analysis

Total RNA from four samples (iPSCs of U1, iPSCs of U1 differentiated for 1 month, and human TM cells of donors 4 and 5) was isolated with TRIzol. The concentration and purity of RNA were determined by measuring the absorbance at 260 and 280 nm (A260/280) using a NanoDrop spectrophotometer (Thermo Fisher Scientific). cDNAs were generated from RNAs through random primed reverse transcription reaction (Promega, Madison, WI). The target genes were amplified in triplicate using the SYBR Green system (Bio-Rad, Hercules, CA). The primers used for amplifying the target genes are listed in Table 1, and *GAPDH* (Gene ID: 2597, OMIM: 138400) was used as a reference gene. PCR reactions were carried out at 95°C for 15 minutes, followed by 50 cycles at 95°C for 10 seconds, at 50°C for 30 seconds, and at 72°C for 30 seconds.

Immunohistochemistry

Cells were grown on coverslips coated with poly-D-lysine (Solarbio Science and Technology, Beijing, China). After reaching 70% to 80% confluency, cells were fixed with 4% paraformaldehyde (Thermo Fisher Scientific), rinsed in Dulbecco's PBS (145-mM NaCl, 8.1-mM $Na_2HPO_4{\cdot}12H_2O$, and 1.9-mM $NaH_2PO_4{\cdot}2H_2O$, pH 7.2–7.4; Thermo Fisher Scientific) for 5 minutes and incubated in the blocking solution (Dulbecco's PBS with 1% bovine serum albumin Sigma-Aldrich) for 1 hour. The sections were further incubated with the diluted primary antibodies (1:100) and the corresponding secondary antibodies (1:200). The nuclei of the tissue were stained with 4′,6-diamidino-2-phenylindole (DAPI; Santa Cruz Biotechnology, Dallas, TX). Coverslips were then mounted on the slides using Neutral Balsam (Solarbio, Beijing, China) and imaged with confocal microscopy (Nikon, Tokyo, Japan). The primary antibodies included rabbit polyclonal antibodies anti-laminin A4 (LAMA4) (Abcam, Cambridge, UK), anti-tissue inhibitor of matrix proteases 3 (TIMP3) (Abcam), anti-aquaporin 1 (AQP1) (Abcam), anti-MYOC (Abcam), mouse polyclonal antibodies anti-collagen IV (ColIV) (Abcam), and Phalloidin-iFluor 488 (Thermo Fisher Scientific). The secondary antibodies included Donkey anti-Rabbit IgG Alexa Fluor 350 and Donkey anti-Mouse IgG Alexa Fluor 488 (Thermo Fisher Scientific).

Induction of Cross-Linked Actin Network Formation

Human differentiated iPSCs and TM cells were exposed to 100-nM DEX for 3 days. Dimethylsulfoxide (Sigma-Aldrich) with the same dilution ratio was used as the vehicle control. High-magnification (100×) images of cells stained with Phalloidin-iFluor 488 were

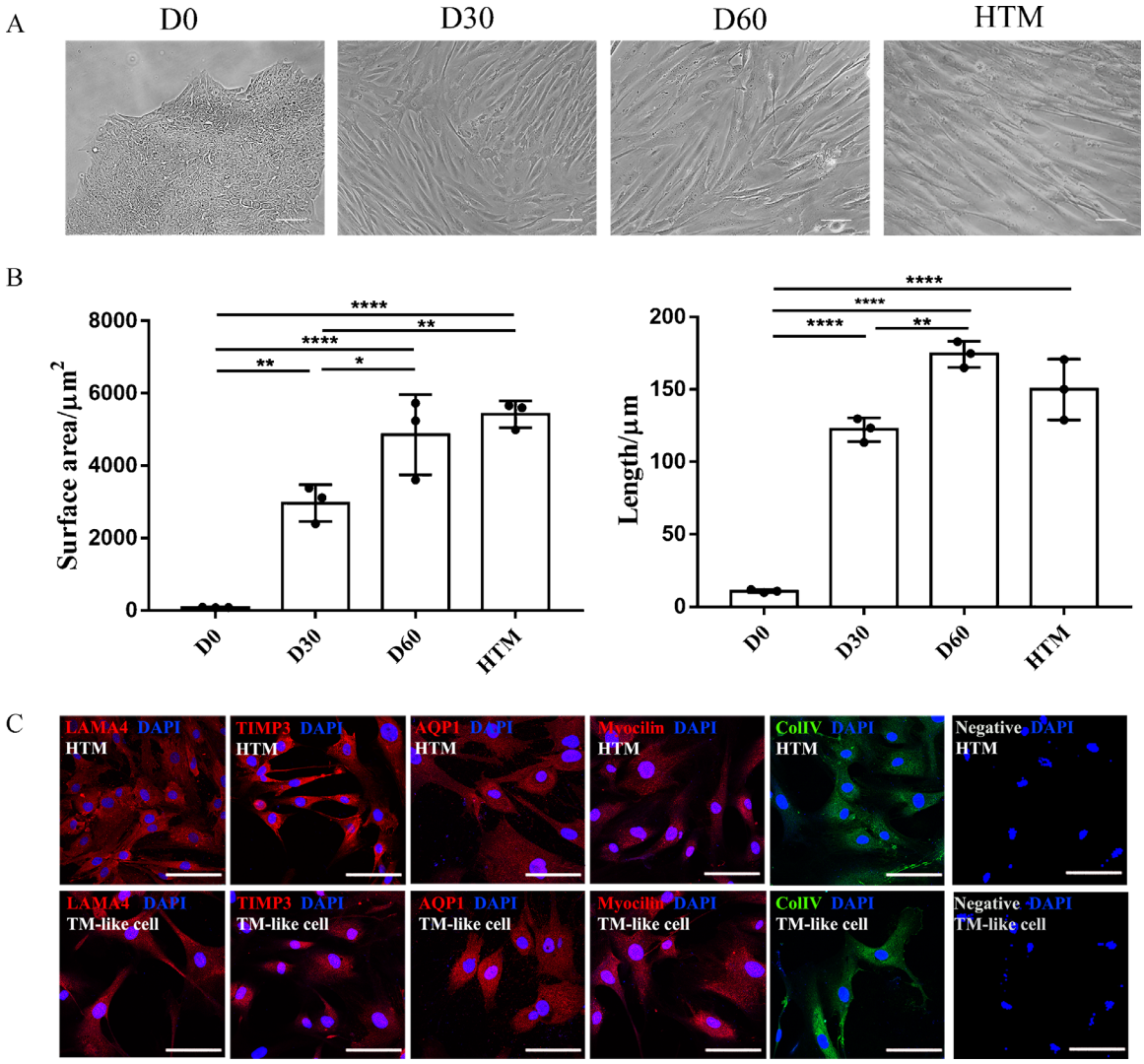

Figure 1. Characterization of human TM-like cells induced by the conditioned medium. (**A**) Morphological observations of TM-like cells during differentiation. Human iPSCs colonies of U1 were generated via reprogramming renal urethra epithelial cells. Through co-culturing with HTM cells, iPSCs were differentiated for 60 days. The morphological changes monitored by Nikon microscopy were compared with HTM cells of donor 1. (**B**) Surface area and length of TM progenitor and TM-like cell. TM progenitors (D30) were significantly smaller than TM-like cells (D60). Tukey's multiple comparisons test was used for data analysis. *$P < 0.05$, **$P < 0.01$, ***$P < 0.001$, ****$P < 0.0001$. (**C**) Immunohistochemical characterization of TM-like cells differentiated for 60 days. Laminin A4 (LAMA4), tissue inhibitor of matrix proteases 3 (TIMP3), aquaporin 1 (AQP1), myocilin (MYOC), and collagen type IV (ColIV) were detected with robust expression in both TM-like cells and HTM cells. *Scale bar*: 100 μm.

taken by confocal microscopy (Nikon). As reported before,[23,24] cross-linked actin networks (CLANs) were defined as a specific cytoskeletal structure with geodesic dome-like polygonal lattices in the dome-shaped cells. CLAN-formed cells in 16 regions of each image were counted. The CLAN forming ratio was calculated by dividing the numbers of cells with the typical CLAN structure by the numbers of the nuclei stained with DAPI.

Statistical Analyses

Two-tailed *t*-tests and normality and log-normal tests were used for statistical analyses. Tukey's multiple comparisons test was used for statistical analysis of cell size data, RT-PCR results, and FPKM values of RNA sequencing. $P < 0.05$ was considered to be statistically significant. Data are expressed as the mean ± standard error of the mean.

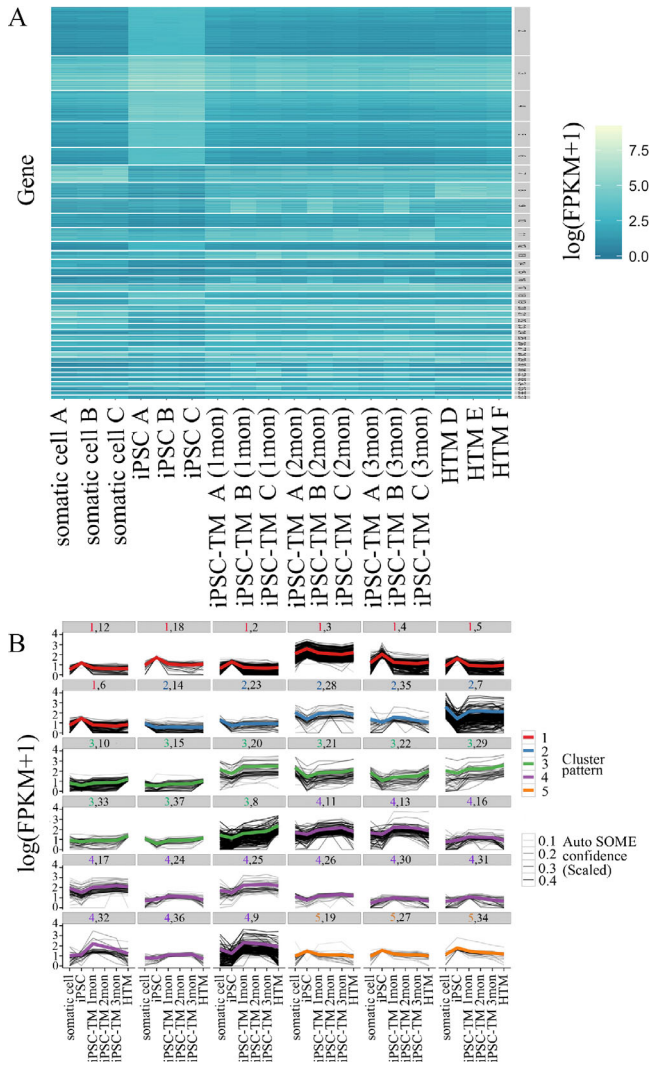

Figure 2. AutoSOME clustering analysis of RNA sequencing data. (**A**) A clustering heat map with the values of log(FPKM + 1). The heat map is ordered from top to bottom by decreasing cluster size and hierarchically ordered from left to right by whole-transcriptome expression. Cell samples were hierarchically ordered as somatic cells used for reprogramming; iPSCs; differentiated iPSCs for 1, 2, and 3 months; and HTM cells. A total of 6300 genes were clustered into 136 clusters based on their expression modulus; 36 clusters remained after removing clusters with more than 500 or fewer than 30 genes. (**B**) Grouping analysis of representative clusters with the same expression pattern. The 136 clusters with the same expression pattern were categorized into five groups, designated as 1 (*red*), 2 (*blue*), 3 (*green*), 4 (*purple*), and 5 (*yellow*). Representative clusters in each group are shown, and the cluster numbers are labeled on the top of each image (e.g., clusters 12, 18, 2, 3, 4, 5, and 6 in group 1). The *black line* represents the log(FPKM + 1) of each gene, and the confidence scale for each gene is reflected by the size of the *black line*. The *colored line* represents the mean value of log(FPKM + 1) in each cluster.

Results

Two Distinct Stages Involved in Human iPSC Differentiation to Trabecular Meshwork Cells

As we described earlier,[9,10,13] human iPSCs reprogrammed from fibroblasts or keratinocytes can be successfully induced to differentiate into cells that resemble TM cells by using medium conditioned by human TM cells. Here, we induced human iPSCs derived from renal epithelial cells to differentiate into TM-resembling cells by using the same approach. Undifferentiated iPSCs were observed as compact colonies comprised of cells with a large nucleus and less cytoplasm. iPSCs differentiated for 1 month altered their morphology to assume a spindle-like shape reminiscent of HTM cells, although their size was much smaller than that of HTM cells (surface area, $P < 0.01$) (Figs. 1A, 1B). In the following 2 months, differentiated cells kept growing (surface area, 5684.0 ± 388.6 μm^2; length, 221.4 ± 6.7 μm) until they reached a similar size as the HTM cells of donor 4 (surface area, 5978.0 ± 372.0 μm^2; length, 200.4 ± 9.0 μm), donor 5 (surface area, 5194.0 ± 320.7 μm^2; length, 158.4 ± 9.6 μm), and donor 6 (surface area, 5292.0 ± 299.5 μm^2; length, 137.6 ± 4.7 μm) (Fig. 1B). We also observed cell growth rate during differentiation (Supplementary Fig. S1). From iPSCs to TM progenitors (D0 to D30), cells were dramatically enlarged at a length-increasing rate of 18.4 μm/day. In the following month (D30 to D60), the cell growth rate (length-increasing rate of 11.6 μm/day) was more reduced than during the first stage (D0 to D30). Therefore, two distinct differentiation stages can be defined in iPSC differentiation: iPSCs to TM progenitors (1 month) and progenitors to TM-like cells (2 months). Our immunohistochemistry analysis showed robust expression of the TM markers LAMA4, TIMP3, AQP1, MYOC, and ColIV in both TM-like cells and human TM cells (Fig. 1C).

Receptors With the Most Robust Expression at Each Differentiation Stage

The observation that iPSC differentiation occurs in two stages is also supported by our previous study, which suggested that differentiated iPSCs display a very stable transcriptional signature after induction for 1 month.[9] Given the roles of the conditioned medium in iPSC differentiation, receptors were assumed to function importantly to transduce the differentiation signals. In this study, we reanalyzed the data to identify highly expressed receptors in each stage of iPSC differentiation through AutoSOME analysis (Fig. 2A). After removing genes with fold change less than 4 and

mean FPKM less than 1,6300 genes were submitted to AutoSOME. Genes were grouped into one of 136 clusters based on similarity of expression modulus and were further classified into five groups based on the gene expression pattern (Fig. 2B). In each group, the black line in the figure represents the log(FPKM + 1) value, and the confidence scale for each gene was reflected by the size of the line. The colored line in each group represents the mean value of log(FPKM + 1). As shown in Figure 2B, genes in groups 2 and 3 were considered to have the highest expression in TM progenitors and human TM cells, respectively.

Through Gene Ontology analysis (http://www.pantherdb.org/), receptors in groups 2 and 3 were selected (Table 1), and their function in stem cell differentiation or TM maintenance was investigated by searching publications in PubMed (Table 2). As shown in Table 2, TGF-β receptor 1 (TGFBR1), receptor-type tyrosine-protein phosphatase-like N (PTPRN), and erythropoietin receptor associated with differentiation at stage 1 have been described as highly relevant to multiple types of stem cell differentiation. Prostaglandin receptors (PTGER and PTGFR), epidermal growth factor receptors (multiple epidermal growth factor-like-domains 9 [MEGF9] and EGF-like repeat and discoidin I-like domain-containing protein 3 [EDIL3]), and TGF-β receptors (TGFBR2 and 3) involved in the differentiation at stage 2 have been shown to play important roles in maintaining the function of the trabecular meshwork.

Confirmation of Expression Modulus of the Selected Receptors by RT-PCR Analysis

We next determined the mRNA levels of these receptors in iPSCs of U1, U1-derived TM progenitor (1 month), and human TM cells of donor 4 and 5 by RT-PCR analysis. GAPDH was determined to be a better reference gene compared with 18S ribosomal RNA (18S) and actin beta (ACTB) through NormFinder analysis (Supplementary Fig. S2)[89] and was used as the reference gene in this study. Overall, the expression of receptors—human erythropoietin receptor (HEPOR), human TGF-β receptor 1 (HTGFBR1), HTGFBR2, HTGFBR3, PTPRN, MEGF9, prostaglandin F2-alpha receptor (PTGFR), EDIL3, and prostaglandin E receptors 1, 2, and 4 (PTGER1, 2, and 4)—in TM progenitors and human TM cells was higher than in iPSCs (Fig. 3). As expected, receptors with the highest FPKM values (Supplementary Fig. S3) were also detected with the highest expression in HTM cells by RT-PCR. However, receptors with the highest FPKM values in TM progenitors (HTGFBR1, HEPOR, and PTPRN) were not identified as being the most robustly expressed receptors in U1-derived TM progenitors.

Xeno- and Feeder-Free Differentiation With Recombinant Cytokines

To determine the effects of the selected receptors on stem cell differentiation, recombinant cytokine ligands were purchased and used for iPSC differentiation (Table 3). After multiple tests, an optimal two-stage protocol was determined based on cell viability and morphology (Fig. 4A). The first stage is to induce iPSCs to differentiate for 7 days in the presence of TGF-β_1, NGF-β, and EPO. The second stage is to generate TM-resembling cells by using PGF2α and EGF for another 14 days. We first detected the cytokine concentrations in the conditioned medium by ELISA assay. As shown in Figure 4B, the ELISA results demonstrated a detectable supernatant concentration of TGF-β_1 (37.9 $\pm$ 3.2 pg/mL), NGF-β (45.8 $\pm$ 4.9 pg/mL), EPO (40.6 $\pm$ 0.7 pg/mL), EGF (54.3 $\pm$ 1.4 pg/mL), and PGF2α (39.4 $\pm$ 7.0 pg/mL). This observation indicated that these cytokines (TGF-β_1, NGF-β, EPO, EGF, and PGF2α) are retained at detectable levels in HTM conditioned media and might be important for iPSC differentiation.

The morphological changes induced by this new protocol are similar to those observed using the traditional approach (Fig. 1A), including the generation of TM progenitors with a spindle-like shape and a smaller size (surface area, $P < 0.0001$; length, $P < 0.0001$) (Fig. 5B), progressing toward TM resembling morphology (Fig. 5B). Additionally, human iPSCs derived from different individuals (U1, U2, or U3) all displayed the same morphological changes during the differentiation (Fig. 5B).

Characterization of iPSC-Derived TM Cells

As described previously,[90,91] TM cells had a high expression of LAMA4, TIMP3, AQP1, MYOC, and ColIV and a capacity to form DEX-inducible CLANs. Immunohistochemistry analysis indicated that the differentiated iPSCs of U1, U2, and U3 using recombinant cytokines expressed high levels of LAMA4, TIMP3, AQP1, MYOC, and ColIV (Fig. 6A), similar to TM-like cells generated by using the conditioned medium (Fig. 1B). Additionally, DEX-inducible CLAN formation can be observed in TM-like cells generated using the new approach. As shown in Figure 6B, a significantly higher percentage of CLAN formation can be observed in DEX-treated differentiated

Table 2. Receptors Associated With iPSC Differentiation

	Gene ID		FPKM/Average				Literatures (TITLE/ABSTRACT must include the keywords)		Literature (IF is in the top 5)	
Cell Type	Full Name	Abbreviation	iPSC	TM Progenitor	HTM	Keywords	Stem Cell Differentiation	Trabecular Meshwork	Stem Cell Differentiation	Trabecular Meshwork
TM progenitor	Receptor-type tyrosine-protein phosphatase-like N	PTPRN	3.7	49.1	0.4	Phosphatase	176	34	Chan et al. 2003,[25] Cornejo et al. 2011,[26] Firulli et al. 2003,[27] Yasui et al. 2014,[28] Yu et al. 2013.[29]	Buie et al. 2013,[30] Hosseini et al. 2006,[31] Luo et al. 2014,[32] Nishida et al. 1994,[33] Pattabiraman, Pecen, and Rao 2013,[34] Ramachandran et al. 2011,[35] Sawaguchi et al. 1994,[36] Tellios et al. 2017,[37] Thomson et al. 2019,[38] Xue, Comes, and Borras 2007,[39] Xue et al. 2006,[40] Zaiden and Beit-Yannai 2015.[41]
	TGF-beta receptor type-1	TGFBR1	23.5	56.4	12.3	Transforming growth factor	97	136	Bonauer et al. 2009,[42] Jia et al. 2017,[43] Wandzioch and Zaret 2009,[44] Xu et al. 2002,[45] Zhang et al. 2015.[46]	Agarwal and Agarwal 2018,[47] Gabelt and Kaufman 2005,[48] Liton et al. 2005; Luna et al. 2011,[49] Raghunathan et al. 2015,[50] Tamm 2002,[51] Wahlig, Lovatt, and Mehta 2018.[52]
	Erythropoietin receptor	EPOR	4.6	11.8	3.1	Erythropoietin	22	1	Suda et al. 1985,[53] Nakahata et al. 1985,[54] Papayannopoulou et al. 1979,[55] Greenberger et al. 1983,[56] Humphries et al. 1981,[57] Suda et al. 1984.[58]	Wierzbowska et al. 2010.[59]

Table 2. Continued

	Gene ID		FPKM/Average				Literatures (TITLE/ABSTRACT must include the keywords)		Literature (IF is in the top 5)	
Cell Type	Full Name	Abbreviation	iPSC	TM Progenitor	HTM	Keywords	Stem Cell Differentiation	Trabecular Meshwork	Stem Cell Differentiation	Trabecular Meshwork
HTM	TGF-beta receptor type-2	TGFBR2	2.8	50.0	163.2	Transforming growth factor	97	136	Bonauer et al. 2009,[42] Jia et al. 2017,[43] Wandzioch and Zaret 2009,[44] Xu et al. 2002,[45] Zhang et al. 2015.[46]	Agarwal and Agarwal 2018,[47] Gabelt and Kaufman 2005,[48] Liton et al. 2005;Luna et al. 2011,[49] Raghunathan et al. 2015,[50] Tamm 2002,[51] Wahlig, Lovatt, and Mehta 2018.[52]
	Transforming growth factor beta receptor type 3	TGFBR3	2.4	12.6	13.4		97	136		
	Prostaglandin F2-alpha receptor	PTGFR	0.1	2.6	11.4	Prostaglandin	7	105	Ludin et al. 2014,[60] North et al. 2007,[61] Sancilio et al. 2019,[62] Wong et al. 2016,[63] Zhang et al. 2017.[64]	Barraza, McLaren, and Poeschla 2010,[65] Garnock-Jones 2014,[66] Hoy 2018,[67] Impagnatiello et al. 2019,[68] Narayanaswamy et al. 2015.[69]
	Prostaglandin E2 receptor EP4 subtype	PTGER4	0.3	2.5	1.0		7	105		
	EGF-like repeat and discoidin I-like domain-containing protein 3	EDIL3	16.1	77.4	152.4	Integrin	80	46	Cheng et al. 2019,[70] Jiang et al. 2016,[71] Aoyama et al. 1999,[72] Kang et al. 2017,[73] Mikkola et al. 2003,[74] Przybyla, Lakins, and Weaver 2016.[75]	Clark et al. 2013, [76] Faralli, Filla, and Peters 2019,[77] Inoue and Tanihara 2013,[78] Kwon and Tomarev 2011,[79] Yan et al. 2020.[80]
	Multiple epidermal growth factor-like domains protein 9	MEGF9	2.3	4.4	11.5	epidermal growth factor	29	7	Kratchmarova et al. 2005,[81] Moore et al. 1997,[82] Nakajima et al. 2007,[83] Prabhakaran, Venugopal, and Ramakrishna 2009,[84] Zhou et al. 2016.[85]	Acharya et al. 2012,[86] Wiederholt, Groth, and Strauss 1998,[87] Wordinger et al. 1998.[88]

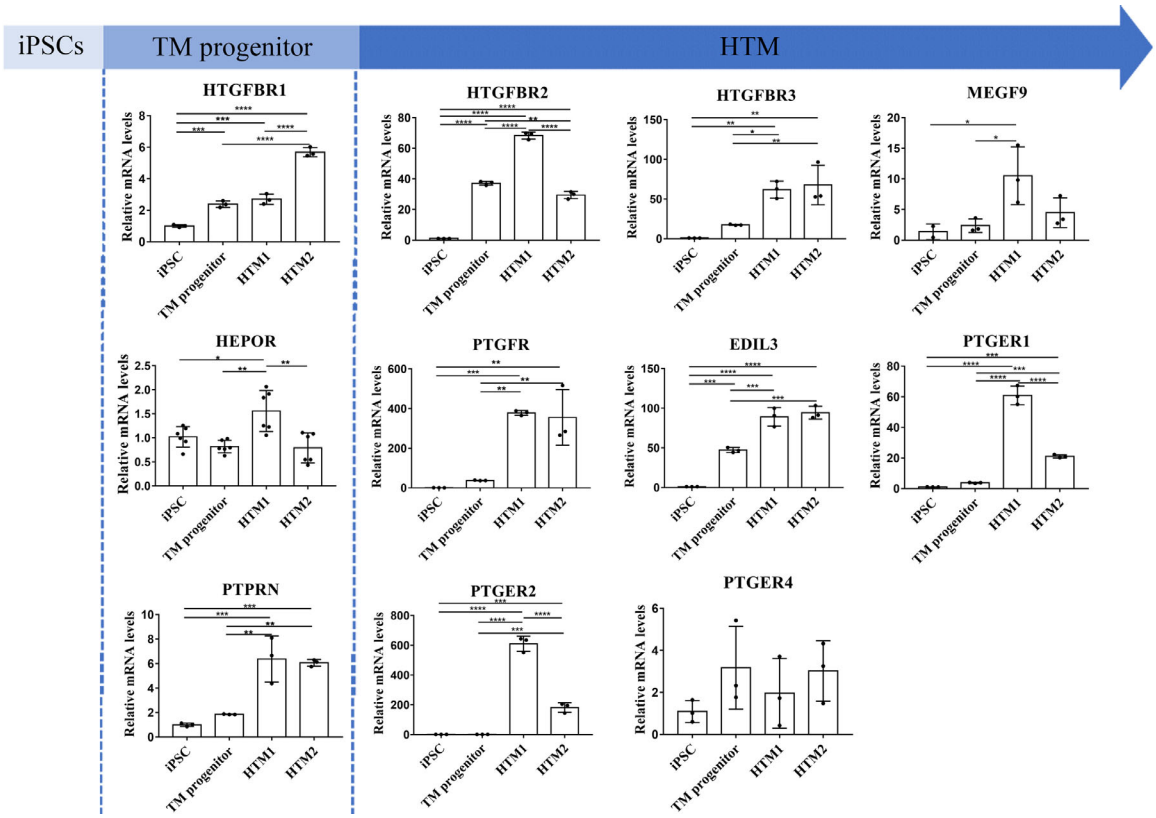

Figure 3. Relative mRNA levels of receptors associated with two-stage differentiation. RT-PCR analysis was used to examine the expression of human transforming growth factor-β receptor 1 (HTGFBR1), human erythropoietin receptor (HEPOR), protein tyrosine phosphatase receptor-type N (PTPRN) for stage 1, human transforming growth factor beta receptor 2 (HTGFBR2), human transforming growth factor beta receptor 3 (HTGFBR3), multiple epidermal growth factor-like-domains 9 (MEGF9), prostaglandin F2 alpha receptor (PTGFR), EGF-like repeat and discoidin I-like domain-containing protein 3 (EDIL3), and prostaglandin E receptors 1, 2, and 4 (PTGER1, 2, and 4) for stage 2. GAPDH was used as the reference gene. Data from three independent experiments ($n = 3$) were statistically analyzed by Tukey's multiple comparisons. *$P < 0.05$, **$P < 0.01$, ***$P < 0.001$, ****$P < 0.0001$.

Table 3. Xeno- and Feeder-Free Differentiation by Recombinant Cytokines

Stage	Medium	Serum	High Receptors	Cytokines	Concentration	Differentiation Period
1	MEM-α	KnockOut Serum Replacement	TGFBR1	TGF-β_1	2 ng/mL	7 d
			PTPRN	NGF-β	100 ng/mL	
			EPOR	Erythropoietin	2 U/mL	
2	MEM-α	KnockOut Serum Replacement	TGFBR2	TGF-β_1	2 ng/mL	14 d
			TGFBR3			
			PTPRN	NGF-β	100 ng/mL	
			EPOR	Erythropoietin	2 U/mL	
			PTGER	PGF2α	10 µM	
			PTGFR			
			MEGF9	EGF	10 ng/mL	
			EDIL3			

iPSCs of U1, U2, and U3 than controls ($P = 0.0013$, $P = 0.0023$, and $P < 0.0001$, respectively), which exhibited a similar percentage as compared with DEX-treated human TM cells of donor 4 (19.69% ± 1.2 %). We further compared the transcriptomics properties of iPSC TM-like cells using two approaches and TM cells. Like our principle component analysis,[9] U1, U2, and U3 TM-like cell-C is a distinct cell type compared with U1, U2, and U3 iPSCs and exhibits a more transcriptional similarity than TM cells (Fig. 6C). However, this

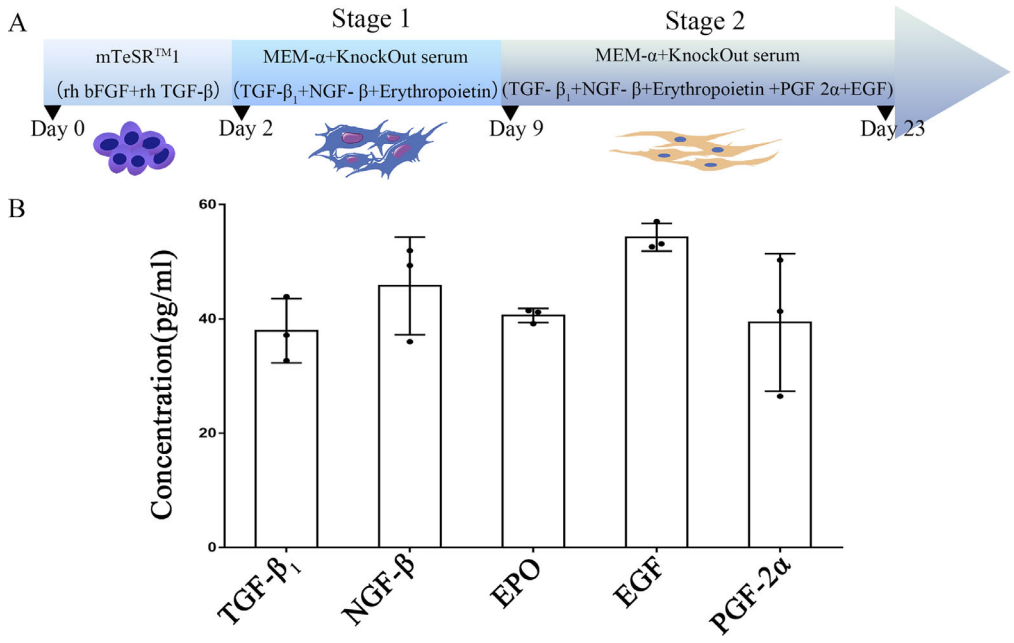

Figure 4. Xeno- and feeder-free differentiation with recombinant cytokines. (**A**) Diagram of the new differentiation approach with two distinct stages. The first stage is to induce iPSCs to differentiate for 7 days by using TGF-β1, NGF-β, and EPO. Two more recombinant cytokines were involved in the differentiation of the second stage (14 days), including PGF2α and EGF. (**B**) ELISA analysis of the cytokines in the medium conditioned by HTM cells. Observable levels of TGF-β_1, NGF-β, EPO, EGF, and PGF2α, as the ligands of the selected receptors, were found in the conditioned medium of HTM cells ($n = 3$). The experiment was repeated three times by using HTM cells of three donors.

new methodology detected only U2 TM-like cells with a transcriptomic similar to that of TM cells. U1 and U3 TM-like cell-X retained a similar molecular property compared with iPSCs.

Discussion

Because the iPSC-derived TM-like cells are a promising cell type to restore IOP hemostasis and AH outflow in glaucoma,[8,92] it is crucial to develop a new differentiation approach to generate TM-like cells that are more feasible for clinical usage. According to our RNA sequencing data (Fig. 2), numerous stem cell fate-related signals are changed (data not shown). We observed that the ligands relevant to these signals would eventually function through binding to the receptors, and the receptors would be controlled by multiple feedback mechanisms to ensure an appropriate level during iPSC differentiation.[93] We thus selected the highly expressed receptors relevant to stem cell differentiation (Table 2) to establish the new methodology. Although RT-PCR results using U1 iPSCs showed some difference compared with previous RNA sequencing data (Fig. 3; Supplementary Fig. S3), new RNA sequencing data using urine-derived iPSCs also exhibited robust expression of HTGFBR1, HEPOR, and PTPRN in TM progenitors and high expression of HTGFBR, MEGF, PTGFR, PTGFR, EDIL3, and PTGER in TM cells (Supplementary Figs. S3 and S4). We thus have established a new methodology with the ligands relative to the above receptors (Fig. 4).

Compared with the traditional approach,[13] we first improved the origin of iPSCs, renal urethra epithelial cells. Compared to dermal fibroblast cells from skin used in our previous study,[8,9] renal urethra epithelial cells are easier to collect from urine and more feasible for use in clinical settings. Additionally, iPSCs are generated through an integration-free approach by Sendai virus carrying Oct4, Sox2, c-Myc, and Klf4 transcription factors. This is particularly important for clinic usage, as this approach avoids the harmful effects of leaky transgene expression and insertional mutagenesis.[94]

Another benefit of this new approach is a shorter differentiation time. Within 1 week undifferentiated iPSCs start to exhibit a TM-resembling morphology with a spindle-like shape (Fig. 5), which is the most critical period for changing cell fate and morphology (Fig. 1).[9] The subsequent stage of differentiation (2 weeks) is mainly responsible for cell growth until the cells reach the same size as HTM cells (Fig. 5). Compared to 2-month differentiation using

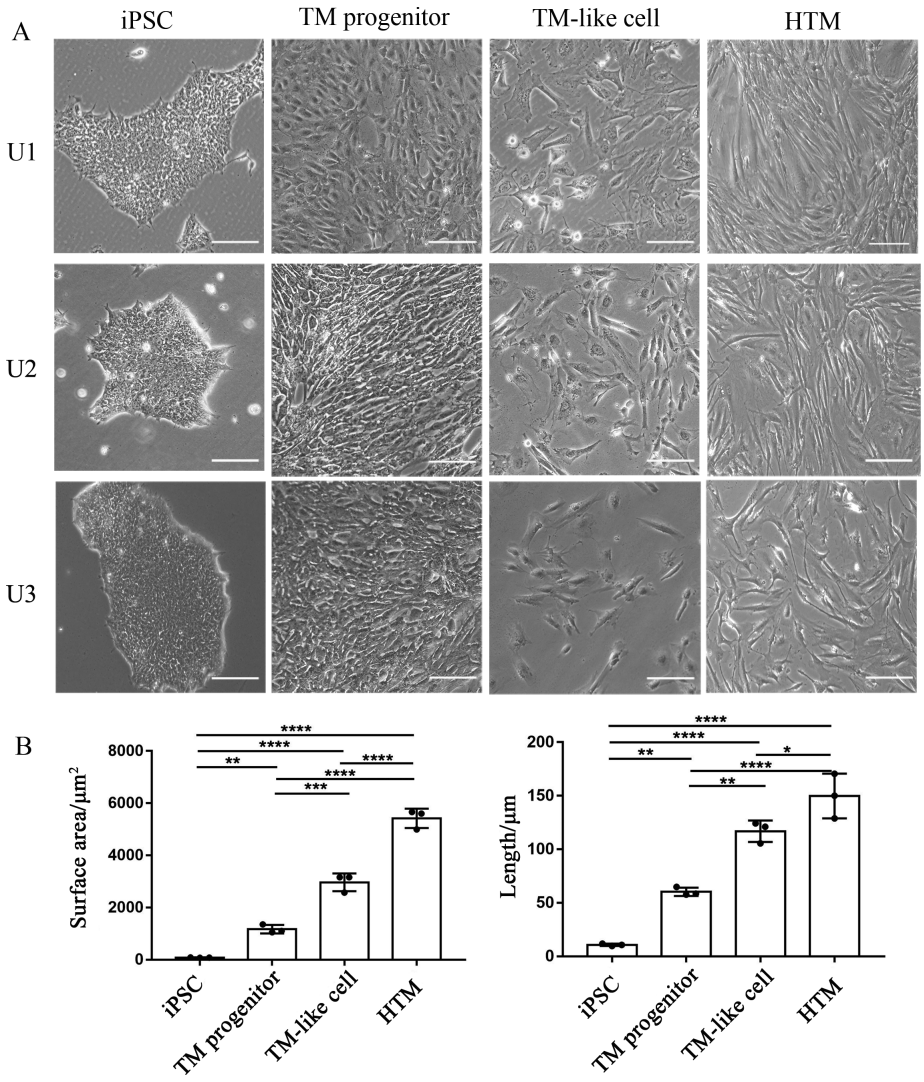

Figure 5. Morphological observations of human TM-like cells induced by cytokines. (**A**) Morphological changes in human iPSCs during differentiation. Human iPSCs from renal urethra epithelial cells of U1, U2, and U3 were differentiated into a TM-resembling cell type using recombinant cytokines. The TM progenitor at stage 1 exhibited a spindle-like shape with a smaller cell size than human TM cells. Cells at stage 2 displayed a TM-like morphology with a similar cell size compared with human TM cells of donors 4, 5, and 6. *Scale bar*: 100 µm. (**B**) Surface area and length of TM-like and HTM cells. TM progenitors were significantly smaller than HTM cells. Tukey's multiple comparisons test was used for data analysis. *$P < 0.05$, **$P < 0.01$, ***$P < 0.001$, ****$P < 0.0001$.

a conditioned medium, the new approach is much more efficient for generating TM-resembling cells. The reason for the accelerated development might be a higher concentration of recombinant cytokines achieved in the new approach compared with the cytokines secreted by human TM cells. Shortening the differentiation period is particularly critical for avoiding the side effects of long-term cell culture, such as cell senescence and genetic mutation.[16,17]

The third vital improvement offered by this new approach is avoiding contamination from bovine serum and human cell cultures. In this study, we used the KnockOut Serum Replacement, a substitute for FBS that contains the essential supplements for iPSCs growth.[19] Additionally, recombinant cytokine use avoids complications resulting from the use of human donor materials, such as media conditioned from human beings. These improvements potentially avoid the variabilities of serum obtained from different batches or among different human donors.

Most importantly, our characterization indicates that TM-like cells are a TM-resembling cell type (Figs. 5 and 6). We also found that the reported TM biomarkers[95] SERPINA3, PTGDS, MYOC, FCGBP, HBB, and HLA-DRA were not only robustly expressed in TM cells but also highly expressed in TM-like cells, whether by the traditional approach or using the cytokine-based approach (Supplementary Fig. S5).

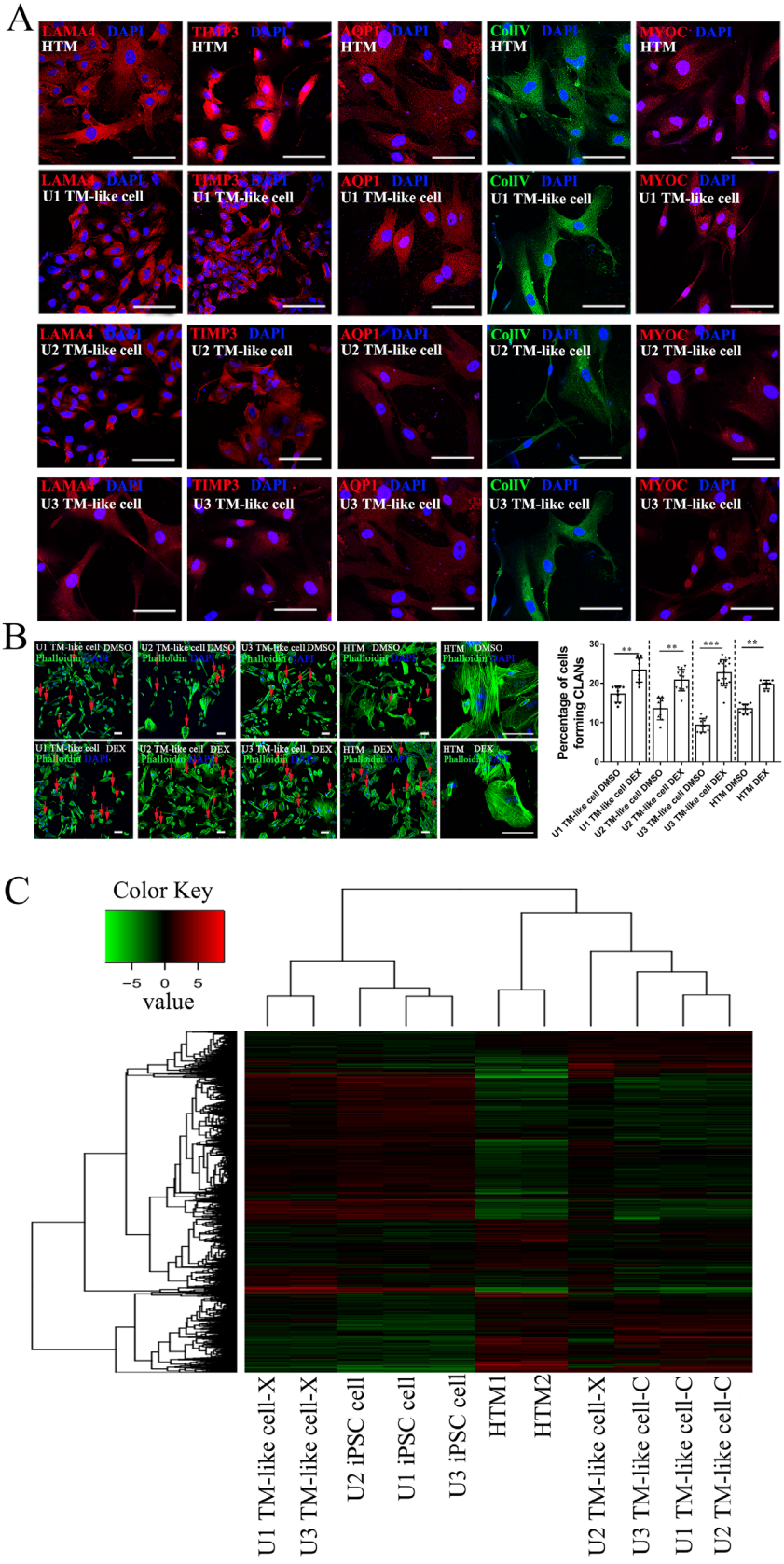

Figure 6. Characterization of TM-like cells derived from the new differentiation approach. (**A**) Immunohistochemical characterization of U1-, U2-, and U3-derived TM-like cells using recombinant cytokines. LAMA4, TIMP3, AQP1, MYOC, and ColIV were detected with robust →

←

expression in both TM-like cells and human TM cells. (**B**) CLAN formation of U1-, U2-, and U3-derived TM-like cells induced by DEX. Differentiated iPSCs of U1, U2, U3, and HTM from donor 4 treated with DMSO or 100-nM DEX were stained with Phalloidin-iFluor 488 (*green*) and DAPI (*blue*). Cells forming CLANs in the representative image of each sample are indicated by the *red arrows* (*left panel*). The percentage of CLAN formation was calculated from 16 images of each sample (*right panel*). One image with a detailed structure of CLANs is shown at a higher magnification. *Scale bar*: 100 µm. Data were statistically analyzed by two-tailed *t*-test. $^{**}P < 0.01$, $^{***}P < 0.001$. (**C**) RNA sequencing was carried out in human urethra epithelial cell-derived iPSCs (U1, U2, and U3), conditioned medium-derived TM-like cells (U1, U2, and U3 TM-like cell-C), TM-like cells by xeno-free approach (U1, U2, and U3 TM-like cell-X), and TM cells (HTM1 and HTM2). Cluster analysis was performed using differentially expressed genes (DEGs) with fold differences ≥ 2 ($|\log_2 FC| \geq 1$) and $P < 0.05$. TM-like cell-C is a distinct cell type relevant to iPSC that exhibits a more transcriptional similarity to TM cells. U2 TM-like cell-X was detected with a transcriptomic similar to that of TM cells, but U1 and U3 TM-like cell-X retained molecular properties similar to those of iPSCs.

The reported TM progenitor biomarkers[95] RPLP0, RAB3B, MARCH4, FOXD1, TSPOAP1, and WDR1 were still detected, with the most robust expression occurring in our TM-like cells. Taken together, our TM-like cells are not progenitor-resembling cells but have greater similarity with TM cells.

We are aware of some possible issues associated with large-scale production of TM-like cells using this approach. Apoptosis during the iPSC differentiation remains a fundamental issue regardless of whether conditioned medium or recombinant cytokines are used. One reason for this may be the withdrawal of leukemia inhibitory factor during differentiation, which has been reported to cause the death of more than 30% of stem cells.[96,97] These apoptotic cells are cells that fail to exit self-renewal.[98] Apoptosis is necessary and benefits stem cell differentiation, which is essential to promoting differentiation efficiency.[99] However, disruption of the balance between survival and death of iPSCs during differentiation can lead to excessive cell viability loss, which can be problematic for large-scale production of TM-like cells. Another issue is the transcriptional difference between urine-derived TM-like cells and HTM cells, despite the success of one donor-derived iPSC differentiation (Fig. 6). This is surprising, as the TM-like cells exhibited a distinct cell morphology compared with stem cell colonies. In view of the differentiation, this might be due to different iPSC viabilities. At the early stage of differentiation, U1 and U3 iPSCs require more time to reach 100% confluency compared with U2. As shown in Supplementary Figure S6, after two-stage differentiation, U1 and U3 TM-like cells exhibited lower confluency than U2-derived cells. Our results suggest that cell viability would be necessary for improving differentiation efficiency using the cytokine-based approach.

Conclusions

This study identified a practical iPSC differentiation approach to generating TM-like cells that is more feasible for clinic usage. We first defined two distinct stages of iPSC differentiation and selected highly expressed receptors at each stage of differentiation, and we have developed a new type of differentiation using the corresponding recombinant cytokines. By using this approach, human iPSCs from three individuals were all successfully differentiated into a TM-like cell type with robust expression of TM markers and the ability for DEX-induced CLAN formation.

Acknowledgments

Supported by grants from the National Key Research and Development Program (2018YFA 0109500), National Natural Science Foundation of China (81870653), Young Taishan Scholars in Shandong Province 2021, Shandong Key Research and Development Program (2019GSF107075), and Shandong Province National Science Foundation (ZR2017BH007).

Disclosure: **W. Wang,** None; **Y. Miao,** None; **S Sui,** None; **Y. Wang,** None; **S. Wu,** None; **Q. Cao,** None; **H. Duan,** None; **X. Qi,** None; **Q. Zhou,** None; **X. Pan,** None; **J. Zhang,** None; **X. Chen,** None; **Y. Han,** None; **N. Wang,** None; **M.H. Kuehn,** None; **W. Zhu,** Qingdao Haier Biotech Co. Ltd. (C)

* WW and YM contributed equally to this work.

References

1. Johnson M. What controls aqueous humour outflow resistance. *Exp Eye Res*. 2006;82:545–557.
2. Quigley HA. Glaucoma. *The Lancet*. 2011;377:1367–1377.
3. Quigley HA, Broman AT . The number of people with glaucoma worldwide in 2010 and 2020. *Br J Ophthalmol*. 2006;90:262–267.

4. Castro A, Du Y. Trabecular Meshwork Regeneration - A Potential Treatment for Glaucoma. *Curr Ophthalmol Rep*. 2019;7:80–88.
5. Yun H, Zhou Y, Wills A, Du Y. Stem Cells in the Trabecular Meshwork for Regulating Intraocular Pressure. *J Ocul Pharmacol Ther*. 2016;32:253–260.
6. Roubeix C, Godefroy D, Mias C, et al. Intraocular pressure reduction and neuroprotection conferred by bone marrow-derived mesenchymal stem cells in an animal model of glaucoma. *Stem Cell Res Ther*. 2015;6:177.
7. Du Y, Yun H, Yang E, Schuman JS. Stem cells from trabecular meshwork home to TM tissue in vivo. *Invest Ophthalmol Vis Sci*. 2013;54:1450–1459.
8. Zhu W, Gramlich OW, Laboissonniere L, et al. Transplantation of iPSC-derived TM cells rescues glaucoma phenotypes in vivo. *Proc Natl Acad Sci USA*. 2016;113:E3492–E3500.
9. Zhu W, Godwin CR, Cheng L, Scheetz TE, Kuehn MH. Transplantation of iPSC-TM stimulates division of trabecular meshwork cells in human eyes. *Sci Rep*. 2020;10:2905.
10. Abu-Hassan DW, Li X, Ryan EI, Acott TS, Kelley MJ. Induced Pluripotent Stem Cells Restore Function in a Human Cell Loss Model of Open-Angle Glaucoma. *Stem Cells*. 2015;33:751–761.
11. Tian YI, Zhang X, Torrejon K, Danias J, Du Y, Xie Y. A Biomimetic, Stem Cell-Derived In Vitro Ocular Outflow Model. *Adv Biosyst*. 2020;4:e2000004.
12. Manuguerra-Gagne R, Boulos PR, Ammar A, et al. Transplantation of mesenchymal stem cells promotes tissue regeneration in a glaucoma model through laser-induced paracrine factor secretion and progenitor cell recruitment. *Stem Cells*. 2013;31:1136–1148.
13. Ding QJ, Zhu W, Cook AC, Anfinson KR, Tucker BA, Kuehn MH. Induction of trabecular meshwork cells from induced pluripotent stem cells. *Invest Ophthalmol Vis Sci*. 2014;55:7065–7072.
14. Dessels C, Potgieter M, Pepper MS. Making the Switch: Alternatives to Fetal Bovine Serum for Adipose-Derived Stromal Cell Expansion. *Front Cell Dev Biol*. 2016;4:115.
15. Keller KE, Bhattacharya SK, Borras T, et al. Consensus recommendations for trabecular meshwork cell isolation, characterization and culture. *Exp Eye Res*. 2018;171:164–173.
16. Kim M, Rhee JK, Choi H, et al. Passage-dependent accumulation of somatic mutations in mesenchymal stromal cells during in vitro culture revealed by whole genome sequencing. *Sci Rep*. 2017;7:14508.
17. Gu Y, Li T, Ding Y, et al. Changes in mesenchymal stem cells following long-term culture in vitro. *Mol Med Rep*. 2016;13:5207–5215.
18. Xue Y, Cai X, Wang L, et al. Generating a non-integrating human induced pluripotent stem cell bank from urine-derived cells. *PloS One*. 2013;8:e70573.
19. Aoshima K, Baba A, Makino Y, Okada Y. Establishment of alternative culture method for spermatogonial stem cells using knockout serum replacement. *PloS one*. 2013;8:e77715.
20. Reda A, Hou M, Winton TR, Chapin RE, Soder O, Stukenborg JB. In vitro differentiation of rat spermatogonia into round spermatids in tissue culture. *Mol Hum Reprod*. 2016;22:601–612.
21. Newman AM, Cooper JB. AutoSOME: a clustering method for identifying gene expression modules without prior knowledge of cluster number. *BMC Bioinform*. 2010;11:117.
22. Parreira VR, Russell K, Athanasiadou S, Prescott JF. Comparative transcriptome analysis by RNAseq of necrotic enteritis Clostridium perfringens during in vivo colonization and in vitro conditions. *BMC Microbiol*. 2016;16:186.
23. Clark AF, Wilson K, McCartney MD, Miggans ST, Kunkle M, Howe W. Glucocorticoid-induced formation of cross-linked actin networks in cultured human trabecular meshwork cells. *Invest Ophthalmol Vis Sci*. 1994;35:281–294.
24. Wade NC, Grierson I, O'Reilly S, et al. Cross-linked actin networks (CLANs) in bovine trabecular meshwork cells. *Exp Eye Res*. 2009;89:648–659.
25. Chan RJ, Johnson SA, Li Y, Yoder MC, Feng GS. A definitive role of Shp-2 tyrosine phosphatase in mediating embryonic stem cell differentiation and hematopoiesis. *Blood*. 2003;102:2074–2080.
26. Cornejo MG, Mabialah V, Sykes SM, et al. Crosstalk between NOTCH and AKT signaling during murine megakaryocyte lineage specification. *Blood*. 2011;118:1264–1273.
27. Firulli BA, Howard MJ, McDaid JR, et al. PKA, PKC, and the protein phosphatase 2A influence HAND factor function: a mechanism for tissue-specific transcriptional regulation. *Mol Cell*. 2003;12:1225–1237.
28. Yasui N, Findlay GM, Gish GD, et al. Directed network wiring identifies a key protein interaction in embryonic stem cell differentiation. *Mol Cell*. 2014;54:1034–1041.

29. Yu WM, Liu X, Shen J, et al. Metabolic regulation by the mitochondrial phosphatase PTPMT1 is required for hematopoietic stem cell differentiation. *Cell Stem Cell*. 2013;12:62–74.
30. Buie LK, Karim MZ, Smith MH, Borras T. Development of a model of elevated intraocular pressure in rats by gene transfer of bone morphogenetic protein 2. *Invest Ophthalmol Vis Sci*. 2013;54:5441–5455.
31. Hosseini M, Rose AY, Song K, et al. IL-1 and TNF induction of matrix metalloproteinase-3 by c-Jun N-terminal kinase in trabecular meshwork. *Invest Ophthalmol Vis Sci*. 2006;47:1469–1476.
32. Luo N, Conwell MD, Chen X, et al. Primary cilia signaling mediates intraocular pressure sensation. *Proc Natl Acad Sci USA*. 2014;111:12871–12876.
33. Nishida K, Kinoshita S, Yokoi N, Kaneda M, Hashimoto K, Yamamoto S. Immunohistochemical localization of transforming growth factor-beta 1, -beta 2, and -beta 3 latency-associated peptide in human cornea. *Invest Ophthalmol Vis Sci*. 1994;35:3289–3294.
34. Pattabiraman PP, Pecen PE, Rao PV. MRP4-mediated regulation of intracellular cAMP and cGMP levels in trabecular meshwork cells and homeostasis of intraocular pressure. *Invest Ophthalmol Vis Sci*. 2013;54:1636–1649.
35. Ramachandran C, Patil RV, Sharif NA, Srinivas SP. Effect of elevated intracellular cAMP levels on actomyosin contraction in bovine trabecular meshwork cells. *Invest Ophthalmol Vis Sci*. 2011;52:1474–1485.
36. Sawaguchi S, Yue BY, Kawa JE, Chang IL, Twining SS, Meberg B. Lysosomal enzyme and inhibitor levels in the human trabecular meshwork. *Invest Ophthalmol Vis Sci*. 1994;35:251–261.
37. Tellios N, Belrose JC, Tokarewicz AC, et al. TGF-beta induces phosphorylation of phosphatase and tensin homolog: implications for fibrosis of the trabecular meshwork tissue in glaucoma. *Sci Rep*. 2017;7:812.
38. Thomson BR, Carota IA, Souma T, Soman S, Vestweber D, Quaggin SE. Targeting the vascular-specific phosphatase PTPRB protects against retinal ganglion cell loss in a pre-clinical model of glaucoma. *Elife*. 2019;8.
39. Xue W, Comes N, Borras T. Presence of an established calcification marker in trabecular meshwork tissue of glaucoma donors. *Invest Ophthalmol Vis Sci*. 2007;48:3184–3194.
40. Xue W, Wallin R, Olmsted-Davis EA, Borras T. Matrix GLA protein function in human trabecular meshwork cells: inhibition of BMP2-induced calcification process. *Invest Ophthalmol Vis Sci*. 2006;47:997–1007.
41. Zaiden M, Beit-Yannai E. Receptor Protein Tyrosine Phosphatase Sigma (RPTP-sigma) Increases pro-MMP Activity in a Trabecular Meshwork Cell Line Following Oxidative Stress Conditions. *Invest Ophthalmol Vis Sci*. 2015;56:5720–5730.
42. Bonauer A, Carmona G, Iwasaki M, et al. MicroRNA-92a controls angiogenesis and functional recovery of ischemic tissues in mice. *Science*. 2009;324:1710–1713.
43. Jia C, Luo B, Wang H, et al. Precise and Arbitrary Deposition of Biomolecules onto Biomimetic Fibrous Matrices for Spatially Controlled Cell Distribution and Functions. *Adv. Mater*. 2017; 29.
44. Wandzioch E, Zaret KS. Dynamic signaling network for the specification of embryonic pancreas and liver progenitors. *Science*. 2009;324:1707–1710.
45. Xu RH, Chen X, Li DS, et al. BMP4 initiates human embryonic stem cell differentiation to trophoblast. *Nat Biotechnol*. 2002;20:1261–1264.
46. Zhang Z, Gupte MJ, Jin X, Ma PX. Injectable Peptide Decorated Functional Nanofibrous Hollow Microspheres to Direct Stem Cell Differentiation and Tissue Regeneration. *Adv Funct Mater*. 2015;25:350–360.
47. Agarwal P, Agarwal R. Trabecular meshwork ECM remodeling in glaucoma: could RAS be a target? *Expert Opin Ther Targets*. 2018;22:629–638.
48. Gabelt BT, Kaufman PL. Changes in aqueous humor dynamics with age and glaucoma. *Prog Retin Eye Res*. 2005;24:612–637.
49. Luna C, Li G, Qiu J, Epstein DL, Gonzalez P. MicroRNA-24 regulates the processing of latent TGFbeta1 during cyclic mechanical stress in human trabecular meshwork cells through direct targeting of FURIN. *J Cell Physiol*. 2011;226:1407–1414.
50. Raghunathan VK, Morgan JT, Chang YR, et al. Transforming Growth Factor Beta 3 Modifies Mechanics and Composition of Extracellular Matrix Deposited by Human Trabecular Meshwork Cells. *ACS Biomater Sci Eng*. 2015;1:110–118.
51. Tamm ER. Myocilin and glaucoma: facts and ideas. *Prog Retin Eye Res*. 2002;21:395–428.
52. Wahlig S, Lovatt M, Mehta JS. Functional role of peroxiredoxin 6 in the eye. *Free Radic Biol Med*. 2018;126:210–220.

53. Suda T, Suda J, Ogawa M. Disparate differentiation in hemopoietic colonies derived from human paired progenitors. *Blood*. 1985;66:327–332.
54. Nakahata T, Tsuji K, Ishiguro A, et al. Single-cell origin of human mixed hemopoietic colonies expressing various combinations of cell lineages. *Blood*. 1985;65:1010–1016.
55. Papayannopoulou T, Kliskalm T, Stamatoyannopoulos G, et al. Cellular regulation of hemoglobin switching: evidence for inverse relationship between fetal hemoglobin synthesis and degree of maturity of human erythroid cells. *Proceedings of the National Academy of Sciences of the United States of America*. 1979;76:6420–6424.
56. Greenberger JS, Sakakeeny MA, Humphries RK, Eaves CJ, Eckner RJ. Demonstration of permanent factor-dependent multipotential (erythroid/neutrophil/basophil) hematopoietic progenitor cell lines. *Proceedings of the National Academy of Sciences of the United States of America*. 1983;80:2931–2935.
57. Humphries RK, Eaves AC, Eaves CJ. Self-renewal of hemopoietic stem cells during mixed colony formation in vitro. *Proceedings of the National Academy of Sciences of the United States of America*. 1981;78:3629–3633.
58. Suda T, Suda J, Ogawa M. Disparate differentiation in mouse hemopoietic colonies derived from paired progenitors. *Proceedings of the National Academy of Sciences of the United States of America*. 1984;81:2520–2524.
59. Wierzbowska J, Robaszkiewicz J, Figurska M, Stankiewicz A. Future possibilities in glaucoma therapy. *Med Sci Mon Int Med J Exp Clin Res*. 2010;16:RA252–RA259.
60. Ludin A, Gur-Cohen S, Golan K, et al. Reactive oxygen species regulate hematopoietic stem cell self-renewal, migration and development, as well as their bone marrow microenvironment. *Antioxid Redox Signal*. 2014;21:1605–1619.
61. North TE, Goessling W, Walkley CR, et al. Prostaglandin E2 regulates vertebrate haematopoietic stem cell homeostasis. *Nature*. 2007;447:1007–1011.
62. Sancilio S, Marsich E, Schweikl H, Cataldi A, Gallorini M. Redox Control of IL-6-Mediated Dental Pulp Stem-Cell Differentiation on Alginate/Hydroxyapatite Biocomposites for Bone Ingrowth. *Nanomaterials (Basel)*. 2019;9.
63. Wong CT, Ussyshkin N, Ahmad E, Rai-Bhogal R, Li H, Crawford DA. Prostaglandin E2 promotes neural proliferation and differentiation and regulates Wnt target gene expression. *J Neurosci Res*. 2016;94:759–775.
64. Zhang N, Chow SK, Leung KS, Cheung WH. Ultrasound as a stimulus for musculoskeletal disorders. *J Orthop Translat*. 2017;9:52–59.
65. Barraza RA, McLaren JW, Poeschla EM. Prostaglandin pathway gene therapy for sustained reduction of intraocular pressure. *Mol Ther*. 2010;18:491–501.
66. Garnock-Jones KP. Ripasudil: first global approval. *Drugs*. 2014;74:2211–2215.
67. Hoy SM. Latanoprostene Bunod Ophthalmic Solution 0.024%: A Review in Open-Angle Glaucoma and Ocular Hypertension. *Drugs*. 2018;78:773–780.
68. Impagnatiello F, Bastia E, Almirante N, et al. Prostaglandin analogues and nitric oxide contribution in the treatment of ocular hypertension and glaucoma. *Br J Pharmacol*. 2019;176:1079–1089.
69. Narayanaswamy A, Leung CK, Istiantoro DV, et al. Efficacy of selective laser trabeculoplasty in primary angle-closure glaucoma: a randomized clinical trial. *JAMA Ophthalmol*. 2015;133:206–212.
70. Cheng ZA, Alba-Perez A, Gonzalez-Garcia C, et al. Nanoscale Coatings for Ultralow Dose BMP-2-Driven Regeneration of Critical-Sized Bone Defects. *Adv Sci (Weinh)*. 2019;6:1800361.
71. Jiang L, Sun Z, Chen X, et al. Cells Sensing Mechanical Cues: Stiffness Influences the Lifetime of Cell-Extracellular Matrix Interactions by Affecting the Loading Rate. *ACS Nano*. 2016;10:207–217.
72. Aoyama K, Oritani K, Yokota T et al. Stromal cell CD9 regulates differentiation of hematopoietic stem/progenitor cells. *Blood*. 1999;93:2586–2594.
73. Kang H, Wong DSH, Yan X, et al. Remote Control of Multimodal Nanoscale Ligand Oscillations Regulates Stem Cell Adhesion and Differentiation. *ACS Nano*. 2017;11:9636–9649.
74. Mikkola HK, Fujiwara Y, Schlaeger TM, Traver D, Orkin SH. Expression of CD41 marks the initiation of definitive hematopoiesis in the mouse embryo. *Blood*. 2003;101:508–516.
75. Przybyla L, Lakins JN, Weaver VM. Tissue Mechanics Orchestrate Wnt-Dependent Human Embryonic Stem Cell Differentiation. *Cell Stem Cell*. 2016;19:462–475.
76. Clark R, Nosie A, Walker T, et al. Comparative genomic and proteomic analysis of cytoskeletal changes in dexamethasone-treated trabecular meshwork cells. *Mol Cell Proteomics*. 2013;12:194–206.
77. Faralli JA, Filla MS, Peters DM. Role of Fibronectin in Primary Open Angle Glaucoma. *Cells*. 2019;8.

78. Inoue T, Tanihara H. Rho-associated kinase inhibitors: a novel glaucoma therapy. *Prog Retin Eye Res*. 2013;37:1–12.
79. Kwon HS, Tomarev SI. Myocilin, a glaucoma-associated protein, promotes cell migration through activation of integrin-focal adhesion kinase-serine/threonine kinase signaling pathway. *J Cell Physiol*. 2011;226:3392–3402.
80. Yan J, Yang X, Jiao X, et al. Integrative transcriptomic and proteomic analysis reveals CD9/ITGA4/PI3K-Akt axis mediates trabecular meshwork cell apoptosis in human glaucoma. *J Cell Mol Med*. 2020;24:814–829.
81. Kratchmarova I, Blagoev B, Haack-Sorensen M, Kassem M, Mann M. Mechanism of divergent growth factor effects in mesenchymal stem cell differentiation. *Science*. 2005;308:1472–1477.
82. Moore KA, Pytowski B, Witte L, Hicklin D, Lemischka IR. Hematopoietic activity of a stromal cell transmembrane protein containing epidermal growth factor-like repeat motifs. *Proc Natl Acad Sci USA*. 1997;94:4011–4016.
83. Nakajima M, Ishimuro T, Kato K, et al. Combinatorial protein display for the cell-based screening of biomaterials that direct neural stem cell differentiation. *Biomaterials*. 2007;28:1048–1060.
84. Prabhakaran MP, Venugopal JR, Ramakrishna S. Mesenchymal stem cell differentiation to neuronal cells on electrospun nanofibrous substrates for nerve tissue engineering. *Biomaterials*. 2009;30:4996–5003.
85. Zhou X, Tan M, Nyati MK, Zhao Y, Wang G, Sun Y. Blockage of neddylation modification stimulates tumor sphere formation in vitro and stem cell differentiation and wound healing in vivo. *Proc Natl Acad Sci USA*. 2016;113:E2935–E2944.
86. Acharya M, Sharp MW, Mirzayans F, et al. Yeast two-hybrid analysis of a human trabecular meshwork cDNA library identified EFEMP2 as a novel PITX2 interacting protein. *Mol Vis*. 2012;18:2182–2189.
87. Wiederholt M, Groth J, Strauss O. Role of protein tyrosine kinase on regulation of trabecular meshwork and ciliary muscle contractility. *Invest Ophthalmol Vis Sci*. 1998;39:1012–1020.
88. Wordinger RJ, Clark AF, Agarwal R, et al. Cultured human trabecular meshwork cells express functional growth factor receptors. *Invest Ophthalmol Vis Sci*. 1998;39:1575–1589.
89. Andersen CL, Jensen JL, Orntoft TF. Normalization of real-time quantitative reverse transcription-PCR data: a model-based variance estimation approach to identify genes suited for normalization, applied to bladder and colon cancer data sets. *Cancer Res*. 2004;64:5245–5250.
90. Clark AF, Steely HT, Dickerson JE, et al. Glucocorticoid induction of the glaucoma gene MYOC in human and monkey trabecular meshwork cells and tissues. *Invest Ophthalmol Vis Sci*. 2001;42:1769–1780.
91. Stamer WD, Clark AF. The many faces of the trabecular meshwork cell. *Exp Eye Res*. 2017;158:112–123.
92. Zhu W, Jain A, Gramlich OW, Tucker BA, Sheffield VC, Kuehn MH. Restoration of Aqueous Humor Outflow Following Transplantation of iPSC-Derived Trabecular Meshwork Cells in a Transgenic Mouse Model of Glaucoma. *Invest Ophthalmol Vis Sci*. 2017;58:2054–2062.
93. Heldin CH, Lu B, Evans R, Gutkind JS. Signals and Receptors. *Cold Spring Harbor perspectives in biology*. 2016;8:a005900.
94. Stadtfeld M, Hochedlinger K. Induced pluripotency: history, mechanisms, and applications. *Genes Dev*. 2010;24:2239–2263.
95. Sathiyanathan P, Tay CY, Stanton LW. Transcriptome analysis for the identification of cellular markers related to trabecular meshwork differentiation. *BMC Genomics*. 2017;18:383.
96. Duval D, Reinhardt B, Kedinger C, Boeuf H. Role of suppressors of cytokine signaling (Socs) in leukemia inhibitory factor (LIF) - dependent embryonic stem cell survival. *Faseb J*. 2000;14:1577–1584.
97. Bluguermann C, Romorini L, Evseenko D, et al. Leukemia Inhibitory Factor Increases Survival of Pluripotent Stem Cell-Derived Cardiomyocytes. *J Cardiovasc Transl Res*. 2018;11:1–13.
98. LeBlanc L, Lee BK, Yu AC, et al. Yap1 safeguards mouse embryonic stem cells from excessive apoptosis during differentiation. *Elife*. 2018;7.
99. Bergmann A, Steller H. Apoptosis, stem cells, and tissue regeneration. *Sci Signal*. 2010;3:re8.